Semiconductor Physics, Quantum Electronics & Optoelectronics, 2017. V. 20, N 1. P. 129-136.
doi: https://doi.org/10.15407/spqeo20.01.129

PACS 87.50.W-

Differentiation of Mueller-matrix invariants of biological tissues fibrillar networks with different phase and amplitude anisotropy

A.G. Ushenko[1], A.V. Dubolazov[1], Yu.A. Ushenko[1], L.Ya. Kushnerick[1], M.Yu. Sakhnovskiy[1], V.G. Zhytaryuk[1], I. Lacusta[1], O.G. Prydiy[1], P. Grygorishin[2]
[1]Chernivtsi National University,
2, Kotsyubinsky str., 58012 Chernivtsi, Ukraine
[2]Bukovinian State Medical University,
58000 Chernivtsi, Ukraine; e-mail: a.dubolazov@chnu.edu.ua

Abstract. The work is aimed at investigation of diagnostic efficiency of a new azimuthally stable Mueller-matrix method for analysis of laser autofluorescence coordinate distributions corresponding to biological tissue histological sections. A new model of generalized optical anisotropy observed in biological tissue protein networks has been proposed to study the processes of laser autofluorescence. The influence of complex mechanisms of both phase anisotropy (linear birefringence and optical activity) and linear (circular) dichroism has been taken into account. The interrelations between the azimuthally stable Mueller-matrix elements characterizing laser autofluorescence and different mechanisms of optical anisotropy have been ascertained. The statistic analysis of coordinate distributions inherent to these Mueller-matrix rotation invariants has been proposed. Thereupon the quantitative criteria (statistic moments of the 1st to 4th orders) of differentiation of histological sections of uterus wall tumor – group 1 (dysplasia) and group 2 (adenocarcinoma) have been found.

Keywords: fluorescent biopsy, biological tissues, malignant tumors of uterus.

Manuscript received 01.11.16; revised version received 17.01.17; accepted for publication 01.03.17; published online 05.04.17.

1. Introduction

Biological tissues can be considered as structurally heterogeneous optical anisotropic media with absorption. To describe interactions of polarized light with these complex systems, more generalized approximations are required, for instance, those based on Mueller-matrix formalism. Nowadays many practical techniques based on the measurement and analyses of Mueller matrices corresponding to the investigated samples are applied in biological and medical researches [1-5]. A separate direction – laser polarimetry – was formed within matrix optics in recent 10-15 years [6-10].

In parallel to polarimetric methods, the fluorescence ones are actively developed. These methods are grounded on diagnostic application of fluorescence effects related with protein molecules and their complexes. Consequently, the valid results concerning the cancer fluorescence diagnostic of cavitary organs were obtained [11-16].

In this research, the model of generalized optical anisotropy inherent to the tissues of women's reproductive sphere is suggested, and on its basis the method of Mueller-matrix mapping laser polarization autofluorescence of histological sections of biopsy taken from benign (dysplasia) and malignant (adenocarcinoma) tumors of uterus wall is applied.

2. Brief theory

In this work, we have limited ourselves by consideration of a spectral-selective case – luminescence of optically active porphyrins in biological tissues in red (λ_f = 0.63…0.65 μm) region of spectrum [17-31]. The excitation of autofluorescence was realized using a blue

solid-state laser with the wavelength $\lambda = 0.405$ μm that coincides with the porphyrins maximum absorption.

The following model ideas concerning optical anisotropy of protein networks are used as the basis for the description of laser polarization autofluorescence in biological tissues.

Formation of laser polarization autofluorescence is based on the mechanisms of optically anisotropic absorption (linear and circular dichroism) [18]; fluorescence of porphyrin molecules ("linear" oscillators) and networks formed by them ("elliptical" oscillators) [19] as well as mechanisms of phase anisotropy (linear and circular birefringence) that modulate the fluorescent radiation of protein molecules and their structures. The mentioned scenario can be described by using Mueller-matrix formalism.

2.1. Absorption – Amino acids and polypeptide chains (primary structure of protein) made by them form the fibrillar (secondary structure) protein networks possessing the linear dichroism. Optical manifestations of this mechanism are exhaustively described by the next Mueller matrices:

$$\{\Psi\} = \begin{Vmatrix} 1 & \varphi_{12} & \varphi_{13} & 0 \\ \varphi_{21} & \varphi_{22} & \varphi_{23} & 0 \\ \varphi_{31} & \varphi_{32} & \varphi_{33} & 0 \\ 0 & 0 & 0 & \varphi_{44} \end{Vmatrix}, \text{ where}$$

$$\varphi_{ik} = \begin{cases} \varphi_{12} = \varphi_{21} = (1-\Delta\tau)\cos 2\rho, \\ \varphi_{13} = \varphi_{31} = (1-\Delta\tau)\sin 2\rho, \\ \varphi_{22} = (1+\Delta\tau)\cos^2 2\rho + 2\sqrt{\Delta\tau}\sin^2 2\rho, \\ \varphi_{23} = \varphi_{32} = (1-\Delta\tau)\sin 2\rho, \\ \varphi_{33} = (1+\Delta\tau)\sin^2 2\rho + 2\sqrt{\Delta\tau}\cos^2 2\rho, \\ \varphi_{44} = 2\sqrt{\Delta\tau}. \end{cases} \quad (1)$$

Here, $\Delta\tau = \dfrac{\tau_x}{\tau_y}$, $\begin{cases} \tau_x = \tau\cos\rho \\ \tau_y = \tau\sin\rho \end{cases}$, τ_x, τ_y are absorption coefficients of linearly polarized orthogonal components of the light beam amplitude.

Availability of complex spiral-like structures or their combinations (third-order structure) of polypeptide protein structures forms the circular dichroism. Optical manifestations of this configuration peculiarities are characterized by the Mueller matrix:

$$\{\Phi\} = \begin{Vmatrix} 1 & 0 & 0 & \phi_{14} \\ 0 & \phi_{22} & 0 & 0 \\ 0 & 0 & \phi_{33} & 0 \\ \phi_{41} & 0 & 0 & 1 \end{Vmatrix}, \text{ where}$$

$$\phi_{ik} = \begin{cases} \phi_{22} = \phi_{33} = \dfrac{1-\Delta g^2}{1+\Delta g^2}, \\ \phi_{14} = \phi_{41} = \pm\dfrac{2\Delta g}{1+\Delta g^2}. \end{cases} \quad (2)$$

Here, $\Delta g = \dfrac{g_\otimes - g_\oplus}{g_\otimes + g_\oplus}$, $g_\otimes$, $g_\oplus$ are absorption indices of left- ($\otimes$) and right-hand ($\oplus$) circularly polarized components of light beam amplitude.

2.2. Fluorescence – Polarization appearance of porphyrin fluorescence is characterized by the Mueller matrix considered in [20]

$$\{F\} = \begin{Vmatrix} 1 & F_{12} & 0 & 0 \\ F_{21} & F_{22} & 0 & 0 \\ 0 & 0 & F_{33} & 0 \\ 0 & 0 & 0 & F_{44} \end{Vmatrix}, \text{ where}$$

$$F_{ik} = F_{11}^{-1} \begin{cases} F_{11} = a - b\sin^2\vartheta, \\ F_{12} = F_{21} = -b\sin^2\vartheta, \\ F_{22} = b(1+\cos^2\vartheta), \\ F_{33} = 2b\cos\vartheta, \\ F_{44} = 2c\cos\vartheta. \end{cases} \quad (3)$$

Here, ϑ is a scattering angle; a and b are the interrelated constants for the system of linear oscillators in isotropic medium, defined by the following relations

$$a = 0.5\left(1 + \left\langle\cos^2\varepsilon\right\rangle\right), \quad (4)$$

$$b = 0.25\left(3\left\langle\cos^2\varepsilon\right\rangle - 1\right), \quad (5)$$

where ε is the angle between the emitting dipole and the azimuth of polarization of the exciting beam. There are two experimentally important cases where the theoretical limits of $\left\langle\cos^2\varepsilon\right\rangle$ can be predicted [20]: if the emission and absorption dipoles are collinear $\left\langle\cos^2\varepsilon\right\rangle = 3/5$, and if the emitting dipoles are randomly aligned $\left\langle\cos^2\varepsilon\right\rangle = 1/3$.

The parameter c is undoubtedly related to optical activity. From the classical viewpoint, a "circular oscillator" should be caused by the induced electric and magnetic transition dipole moments being fully parallel or antiparallel and having the same magnitude. Following this description, optically active liquid-crystal molecules are "elliptical oscillators". The limiting values of c for such a system should be $c = 5/16$.

2.3. Phase modulation of fluorescence. Amino acids and polypeptide chains made by them (primary structure of protein) demonstrate optical activity and are characterized by the following matrix operator

$$\{\Omega\}=\begin{Vmatrix}1 & 0 & 0 & 0\\ 0 & \omega_{22} & \omega_{23} & 0\\ 0 & \omega_{32} & \omega_{33} & 0\\ 0 & 0 & 0 & 1\end{Vmatrix}, \text{ where}$$

$$\omega_{ik}=\begin{cases}\omega_{22}=\omega_{33}=\cos 2\gamma,\\ \omega_{23}=-\omega_{32}=\sin 2\gamma.\end{cases} \quad (6)$$

Here, γ is the rotation angle of polarization plane fluorescent radiation.

Fibrillar (secondary structure) protein networks formed by polypeptide chains possess linear birefringence and are exhaustively described by the Mueller matrix

$$\{D\}=\begin{Vmatrix}1 & 0 & 0 & 0\\ 0 & d_{22} & d_{23} & d_{24}\\ 0 & d_{32} & d_{33} & d_{34}\\ 0 & d_{42} & d_{43} & d_{44}\end{Vmatrix}, \text{ where}$$

$$d_{ik}=\begin{cases}d_{22}=\cos^2 2\rho+\sin^2 2\rho\cos\delta,\\ d_{23}=d_{32}=\cos 2\rho\sin 2\rho(1-\cos\delta),\\ d_{33}=\sin^2 2\rho+\cos^2 2\rho\cos\delta,\\ d_{24}=-d_{42}=\sin 2\rho\sin\delta,\\ d_{34}=-d_{43}=\cos 2\rho\sin\delta,\\ d_{44}=\cos\delta.\end{cases} \quad (7)$$

Here, ρ is the direction of fibril's packing, δ – phase shift between linearly-polarized orthogonal components of fluorescent light amplitude.

Considering the effect of all mechanisms of optically anisotropic absorption and phase anisotropy, the Mueller matrix of laser polarization autofluorescence of the protein network inherent to biological tissue can be written as follows

$$\{M\}=\{D\}\{\Omega\}\{F\}\{\Psi\}\{\Phi\}=\begin{Vmatrix}1 & M_{12} & M_{13} & M_{14}\\ M_{21} & M_{22} & M_{23} & M_{24}\\ M_{31} & M_{32} & M_{33} & M_{34}\\ M_{41} & M_{42} & M_{43} & M_{44}\end{Vmatrix}. \quad (8)$$

The analysis of matrix (8) shows that the elements M_{ik} characterize superposition of mechanisms responsible for linear ($\Delta\tau$) and circular (Δg) dichroism; fluorescence of linear ($F_{12;21;22;33}$) and elliptical (F_{44}) oscillators with the following phase modulation of this radiation by optically active molecules (θ) and birefringent (δ) networks of them.

The "information content" of matrix elements is different. The set of elements $M_{i=1;k=1;2;3;4}(F_{12})$ characterizes fluorescence of linear oscillators originated from anisotropic absorption. The elements $M_{i=2;3;k=1;2;3;4}(F_{21;22;33})$ define the phase-modulated (δ,θ) fluorescence of linear oscillators. Finally, the values of elements $M_{i=4;k=1;2;3;4}(F_{21;22;33}, F_{44})$ contain complex information concerning the fluorescence of linear ($F_{21;22;33}$) and elliptical (F_{44}) oscillators in optically anisotropic medium with linear and circular birefringence.

It should be noted that not all elements of matrix (8) are suitable for practical usage. The reason for that consists in azimuthal dependence of most matrix elements – in general, 12 of 16 elements change at rotation of the sample around the probing axis. It is shown in [2, 4] that the following elements of the matrix $\{M\}$, as well as their combinations, are azimuthally stable, independent of the rotation angle (Θ) of the sample

$$\begin{cases}M_{11}(\Theta)=\text{const},\\ M_{14}(\Theta)=\text{const},\\ M_{41}(\Theta)=\text{const},\\ M_{44}(\Theta)=\text{const}.\end{cases} \quad (9)$$

The analysis of the above presented rotation invariants (9) shows that, by measuring

$$\begin{cases}M_{14}=W(F_{12}(a,b),\varphi_{ik}(\Delta\tau),\phi_{ik}(\Delta g)),\\ M_{41}=Q(F_{21;22;33}(a,b),F_{44}(c),\varphi_{ik}(\Delta\tau),\phi_{ik}(\Delta g),d_{ik}(\delta),\omega_{ik}(\theta)),\end{cases}$$

it is possible to obtain separated and azimuthally-stable information about laser polarization fluorescence of linear ($F_{12;21;22;33}$) and elliptical (F_{44}) oscillators, excited by mechanisms of linear and circular dichroism of laser radiation in optically anisotropic biological tissue.

3. Muller-matrix images of biological layers with different types of birefringence

Optically thin (the geometric thickness $d = 30$ μm, attenuation coefficient $\tau < 0.1$) histological sections of postsurgical biopsy of uterus wall tumors of two types were used as objects of investigation:

- benign tumor (dysplasia) – group 1 (21 samples);
- malignant tumor (adenocarcinoma) – group 2 (21 samples).

Histological sections were prepared according to the standard technique by using the freezing microtome.

The measurements of coordinate distributions for Mueller-matrix elements characterizing polarization properties of histological sections taken from uterus wall tumors were performed using the setup of the standard Stokes-polarimeter. The detailed description of the

optical scheme and basic parts of experimental setup were presented in a series of articles [21-28]. In this research, for autofluorescence excitation we used a diode laser with the wavelength $\lambda = 0.405$ μm and power $W =$ 50 μW. For spectral division of polarization fluorescence in front of CCD-camera, an interference filter was placed with the maximal transmission bandpass $\lambda_f =$ 0.63…0.65 μm, which corresponded to intensity of laser polarization autofluorescence maximally achieved under these conditions.

The values of Mueller-matrix rotation invariants (relations (10), (11)) were determined by means of the algorithm

$$\begin{cases} M_{14} = S_1^{\otimes} - 0.5\left(S_1^0 + S_1^{90}\right), \\ M_{41} = 0.5\left(S_4^0 + S_4^{90}\right). \end{cases} \qquad (10)$$

Here $S_{i=1;4}^{0;90;\otimes}$ are the Stokes vector parameters in the points of digital image corresponding to laser polarization autofluorescence of histological sections measured for a series of linearly (0°, 90°) and right-hand circularly polarized ($\otimes$) probing laser beams within the limits of 2D ($m \times n$) ensemble of light-sensitive pixels.

For objective assessment of coordinate distributions of Mueller-matrix rotation invariants $q \equiv \left\{M_{14;41}(m \times n)\right\}_j$, we used the traditional method of statistic analysis. The set of statistic moments of the 1st to 4th orders which characterize distributions q was calculated using the following algorithms

$$Z_1 = \frac{1}{N}\sum_{j=1}^{N}|q|_j,\ Z_2 = \sqrt{\frac{1}{N}\sum_{j=1}^{N}(q)_j{}^2},$$

$$Z_3 = \frac{1}{Z_2{}^3}\frac{1}{N}\sum_{j=1}^{N}(q)_j^3,\ Z_4 = \frac{1}{Z_2{}^4}\frac{1}{N}\sum_{j=1}^{N}(q)_j{}^4, \qquad (11)$$

where N is the number of pixels of CCD-camera.

Figs. 1 and 2 present the series of experimentally measured (relations (10)) spectral-selective ($\Delta\lambda_f$) Mueller-matrix fluorescent images $M_{14;41}(m \times n)$ characterizing laser polarization fluorescence of optically anisotropic histological sections of uterus wall tumor in the group 1 (Fig. 1) and group 2 (Fig. 2).

The analysis of the data obtained shows the common regularity – the non-zero value of all the Mueller matrices elements characterizing polarization fluorescence of histological sections taken from uterus wall tumor. This fact experimentally confirms the model structure of Mueller matrix (8) as superposition of matrix operators that characterize linear and circular dichroism (1), (2), fluorescence of porphyrins ((3)-(5)) and phase modulation of used radiation (6), (7). However, like it was assumed during the model analysis, polarization autofluorescence is the most vividly manifested in coordinate distributions of Mueller-matrix rotation invariants M_{41} and M_{14} of the samples of groups 1 and 2. These distributions (100×100 pix) are illustrated by the series of coordinate dependencies presented in Figs. 3 and 4.

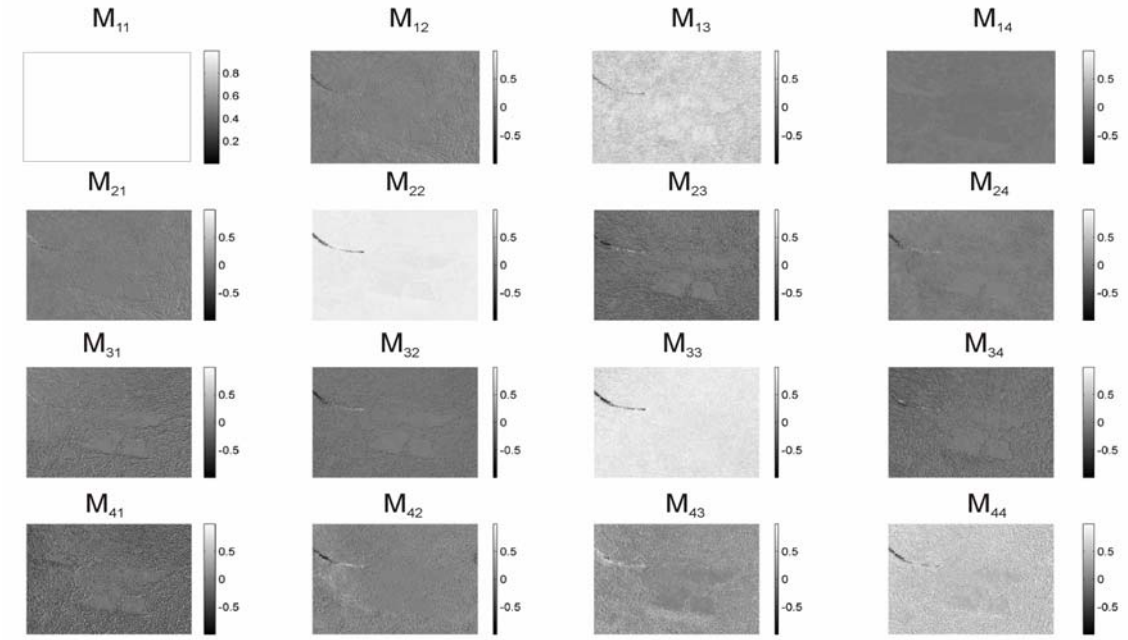

Fig. 1. Mueller-matrix fluorescent images of histological section of benign (dysplasia) tumor of uterus wall (group 1)

Semiconductor Physics, Quantum Electronics & Optoelectronics, 2017. V. 20, N 1. P. 129-136.
doi: https://doi.org/10.15407/spqeo20.01.129

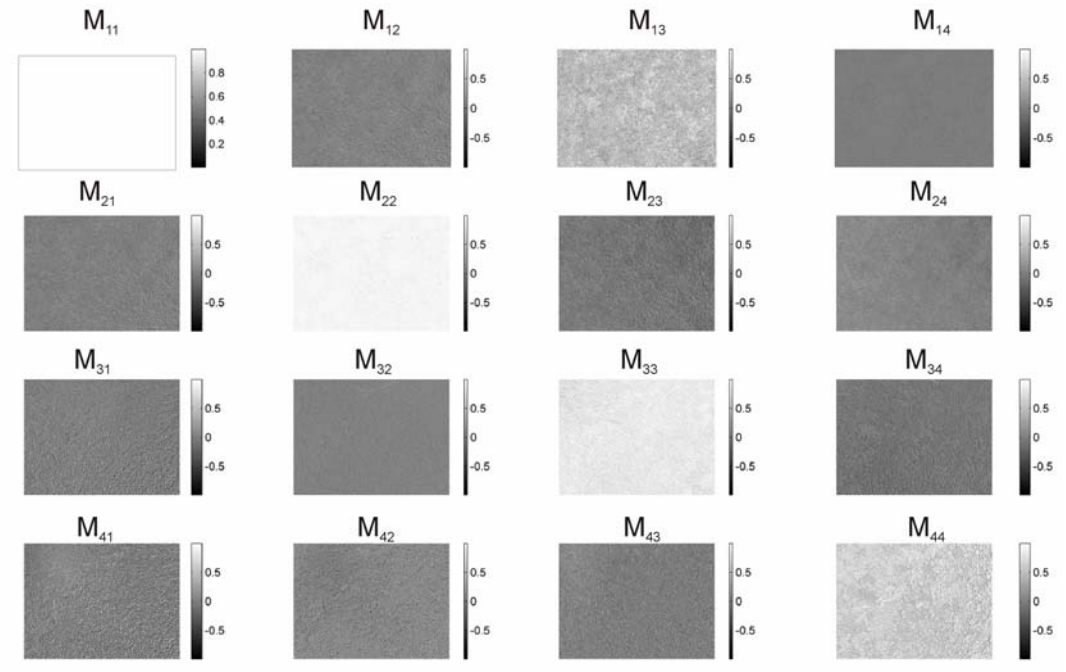

Fig. 2. Mueller-matrix fluorescent images of histological section of malignant (adenocarcinoma) tumor of uterus wall (group 2).

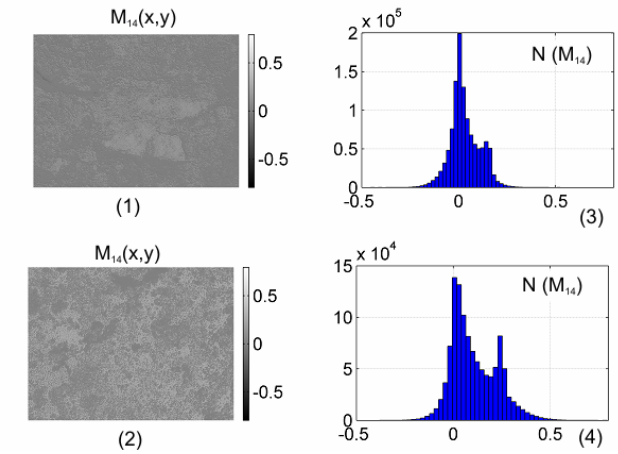

Fig. 3. Coordinate distributions of Mueller-matrix rotation invariant M_{14} for optically thin histological sections of postsurgical biopsy taken from benign (fragments (1), (3)) and malignant (fragments (2), (4)) tumors of uterus wall.

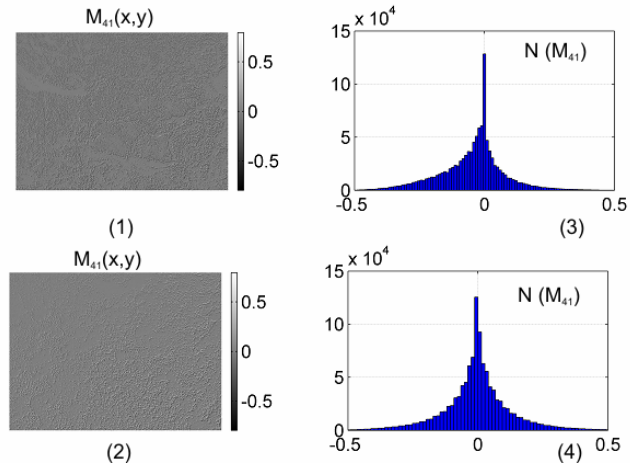

Fig. 4. Coordinate distributions of Mueller-matrix rotation invariant M_{41} for optically thin histological sections of postsurgical biopsy taken from benign (fragments (1), (3)) and malignant (fragments (2), (4)) tumors of uterus wall.

The analysis of coordinate distributions correspondent to the invariant M_{14} (Fig. 3) that characterizes the processes of transformation of circularly polarized fluorescent radiation into the linear one, reveals more than 2-fold decrease of the value ($M_{14}\downarrow$) and the range of changes ($\Delta M_{14}\downarrow$) of this parameter in the plane of tissue histological section with adenocarcinoma (parts 3 and 4).

The inverse situation occurs in the case of Mueller-matrix invariant M_{41} (Fig. 4) that characterizes the processes of transformation of linearly polarized fluorescent radiation into the circular one.

Let us analyze the obtained results from the physical point of view. The samples of both types within the framework of considered model ((1)-(8)) represent the systems of "linear" ($F_{12;21;22;33}(a,b)$) and "elliptic" ($F_{44}(c)$) fluorescent oscillators in the optically-anisotropic matrix with linear (6) and circular (7) birefringence.

As it is well known [21-31], the orientation(ρ)-phase(δ,θ) structure of this matrix depends on physiological (pathological) state of biological tissue. More disordered by directions ($\Delta\rho\uparrow$) birefringent ($\Delta n\approx\text{const}$) fibrillar network is typical for malignant states. On the other hand, in [29-31] it was shown that autofluorescence in the red region of spectrum is increased together with growth and development of tumor. This phenomenon can be related with the liquid-crystal networks of porphyrins that are accumulated in tissues of new malignant formations at different stages of their development.

Thus, the malignant states are accompanied by formation of prevailed, over the disordered "linear" oscillators, system of fluorescent "elliptical" oscillators. *Vice-versa*, in the case of pre-cancer state prevailence of "linear" fluorescent oscillators is more typical. In other words, for tissue with dysplasia the following analytical scenario is realized:

$$\begin{cases} a\uparrow, b\uparrow\rightarrow F_{12;21;22;33}(a,b)\uparrow\Rightarrow M_{14}\Uparrow, \\ c\downarrow\rightarrow F_{44}(c)\downarrow\Rightarrow M_{41}\Downarrow \end{cases}.$$

The inverse regularity takes place for new malignant formations:

$$\begin{cases} a\downarrow, b\downarrow\rightarrow F_{12;21;22;33}(a,b)\downarrow\Rightarrow M_{14}\Downarrow, \\ c\uparrow\rightarrow F_{44}(c)\uparrow\Rightarrow M_{41}\Uparrow. \end{cases}$$

The secondary phase modulation of fluorescent radiation by fibrillar networks of both types samples does not introduce any sufficient changes in the mentioned scenario. As far as for pre-cancer and cancer states it is typical practically the same birefringence ($\Delta n\approx\text{const}$) of protein structures.

The results of the quantitative statistical (relations (11)) analysis of the series of Mueller-matrix rotation invariants of both groups of histological sections are illustrated by the data presented in Table 1.

The following quantitative criteria of differentiation of benign and malignant changes were found after analyzing the mechanisms of laser polarization autofluorescence:

- the Mueller-matrix image $M_{14}(m\times n)$ of a histological section taken from benign tumor is characterized by greater values of statistical moments of the 1st $Z_1(M_{14})$ (2.1 times) and 2nd $Z_2(M_{14})$ (2 times) orders. For statistical moments of higher orders, the reverse tendency is typical – $Z_3(M_{14})$ (2.5 times decrease) and $Z_4(M_{14})$ (2.4 times decrease).
- statistical third-order structures of polypeptide chains of collagen and myosin can be differentiated by the following properties: $Z_1(M_{41})$ – increase by 2.4 times; $Z_2(M_{41})$ – increase by 1.95 times; $Z_3(M_{41})$ – decrease by 3 times and $Z_4(M_{41})$ – decrease by 2 times.

Within both groups of histological sections, by statistical approaches the sensitivity $\left(Se=\frac{d}{d+p}100\%\right)$ and specificity $\left(Sp=\frac{u}{u+h}100\%\right)$ of the technique of Mueller-matrix mapping laser polarization fluorescence of protein networks were determined, where *d* and *p* are the amounts of right and wrong diagnoses within the group 1; *u* and *h* – the same within the group 2.

Table 1. Statistical ($Z_{i=1;2;3;4}$) moments of the 1st to 4th orders distribution for the Mueller-matrix invariants of histological sections taken from uterus wall tumor.

Parameters	M_{14}		M_{41}	
	Dysplasia	Adenocarcinoma	Dysplasia	Adenocarcinoma
Z_1	0.21±0.023	0.12±0.012	0.07±0.01	0.16±0.019
Z_2	0.26±0.039	0.11±0.017	0.10±0.015	0.11±0.036
Z_3	0.82±0.11	2.01±0.24	2.82±0.43	0.74±0.14
Z_4	1.19±0.17	2.47±0.31	3.79±0.53	1.32±0.27

For different Mueller-matrix rotation invariants of laser polarization autofluorescence, the following results were obtained (Table 2).

Table 2. Sensitivity and specificity of the Mueller-matrix technique for mapping the laser polarization fluorescence of the samples taken from uterus wall tumor.

Parameters	M_{14}	M_{41}
$Se(Z_i)$,%	83	92
$Sp(Z_i)$,%	77	86

Thus, the statistical analysis of spectral-selective Mueller-matrix fluorescent invariants proved to be efficient in the task of differential diagnostics of benign and malignant changes in uterus wall.

3. Conclusions

1. The model of laser polarization autofluorescence of biological tissues was suggested, in which the mechanisms of optical anisotropic absorption, autofluorescence and birefringence were taken into consideration.
2. The interrelations between statistical parameters characterizing spectral-selective Mueller-matrix fluorescent images and peculiarities of the mechanisms of porphyrin fluorescence in optically anisotropic histological sections of uterus wall biopsy were found.
3. The efficiency of the method of azimuthally invariant spectral-selective Mueller-matrix mapping laser polarization autofluorescence of protein networks in the task of differentiation of benign and malignant tumors of uterus wall was demonstrated.

Acknowledgement

This work was supported by the grant №0116U001446, №0116U001449, №0115U003241, №0115U003227, №0115U003235 from the Ukraine Foundation for Basic Research.

References

1. Tower T.T., Tranquillo R.T. Alignment maps of tissues: I. Microscopic elliptical polarimetry. *Biophys. J*. 2001. **81**. P. 2954–2963.
2. Smith M.H., Burke P., Lompado A., Tanner E., Hillman L.W. Mueller matrix imaging polarimetry in dermatology. *Proc. SPIE*. 2000. **3991**. P. 210–216.
3. Shribak M. and Oldenbourg R. Techniques for fast and sensitive measurements of two-dimensional birefringence distributions. *Appl. Opt*. 2003. **42**. P. 3009–3017.
4. Smith M.H. Interpreting Mueller matrix images of tissues. *Proc. SPIE*. 2001. **4257**. P. 82–89.
5. Wang X., Wang L.-H. Propagation of polarized light in birefringent turbid media: A Monte Carlo study. *J. Biomed. Opt*. 2002. **7**. P. 279–290.
6. Angelsky O.V., Bekshaev A.Ya., Maksimyak P.P., Maksimyak A.P., Hanson S.G., Zenkova C.Yu. Self-diffraction of continuous laser radiation in a disperse medium with absorbing particles. *Opt. Exp*. 2013. **21**, No. 7. P. 8922–8938.
7. Angelsky O.V., Bekshaev A.Ya., Maksimyak P.P., Maksimyak A.P., Hanson S.G., Zenkova C.Yu. Self-action of continuous laser radiation and Pearcey diffraction in a water suspension with light-absorbing particles. *Opt. Exp*. 2014. **22**, No. 3. P. 2267–2277.
8. Angelsky O.V., Bekshaev A.Ya., Maksimyak P.P., Maksimyak A.P., Hanson S.G. Measurement of small light absorption in microparticles by means of optically induced rotation. *Opt. Exp*. 2015. **23**, No. 6. P. 7152–7163.
9. Ushenko A.G. Polarization correlometry of angular structure in the microrelief pattern of rough surfaces. *Optics and Spectroscopy*. 2002. **92**. P. 227–229.
10. Angelsky O.V., Besaha R.N., Mokhun A.I., Mokhun I.I., Sopin M.O., Soskin M.S., Vasnetsov M.V. Singularities in vectoral fields. *Proc. SPIE*. 1999. **3904**. P. 40.
11. Bard M.P., Amelink A., Skurichina M., Noordhoek V., Hegt R., DuinP., Sterenborg H.J., Hoogsteden H.C., Aerts J.G. Optical spectroscopy for the classification of malignant lesions of the bronchial tree. *Chest*. 2006. **129**. P. 995–1001.
12. Kamath A.V., Chhajed P.N. Role of bronchoscopy in early diagnosis of lung cancer. *J. Chest Dis. Allied Sci.* 2006. **48**. P. 265–269.
13. Grossweiner L.I., Blum A., Goyal G.C. Photophysics and photochemistry of hematoporphyrin, hematoporphyrin derivative and uroporphyrin I. *Advances in Experimental Medicine and Biology*. *Methods in Porphyrin Photosensitization*. 1985. **193**. P. 181–192.
14. Savenkov S.N., Marienko V.V., Oberemok E.A., Sydoruk O.I. Generalized matrix equivalence theorem for polarization theory. *Phys. Rev. E*. 2006. **74**. P. 605–607.
15. Arteaga O., Nichols S., Kahr B. Mueller matrices in fluorescence scattering. *Opt. Lett*. 2012. **37**. P. 2835–2837.
16. Angel'skii O.V., Ushenko A.G., Arkhelyuk A.D., Ermolenko S.B., Burkovets D.N. Structure of matrices for the transformation of laser radiation by biofractals. *Quantum Electronics*. 1999. **29**, No. 12. P. 1074–1077.
17. Ushenko V.A., Sidor M.I., Marchuk Y.F., Pashkovskaya N.V., Andreichuk D.R. Azimuth-invariant Mueller-matrix differentiation of the optical anisotropy of biological tissues. *Optics and Spectroscopy*. 2014. **117**, No. 1. P. 152–157.

18. Ushenko V.A., Zabolotna N.I., Pavlov S.V., Burcovets D.M., Novakovska O.Yu. Mueller-matrices polarization selection of two-dimensional linear and circular birefringence images. *Proc. SPIE*. 2013. **9066**, Eleventh International Conference on Correlation Optics. P. 90661X.
19. Ushenko V.A., Gorsky M.P. Complex degree of mutual anisotropy of linear birefringence and optical activity of biological tissues in diagnostics of prostate cancer. *Optics and Spectroscopy*. 2013. **115**, No. 2. P. 290–297.
20. Ushenko Yu.A., Gorsky M.P., Dubolazov A.V., Motrich A.V., Ushenko V.A., Sidor M.I. Spatial-frequency Fourier polarimetry of the complex degree of mutual anisotropy of linear and circular birefringence in the diagnostics of oncological changes in morphological structure of biological tissues. *Quantum Electronics*. 2012. **42**, No. 8. P. 727.
21. Ushenko V.A. Complex degree of mutual coherence of biological liquids. *ROMOPTO International Conference on Micro- to Nano-Photonics III.* International Society for Optics and Photonics, 2013. P. 88820V–88820V.
22. Ushenko Yu.O., Dubolazov O.V., Karachevtsev A.O., Gorsky M.P., Marchuk Y.F. Wavelet analysis of Fourier polarized images of the human bile. *Appl. Opt.* 2012. **51**, No. 10. P. C133–C139.
23. Ushenko Yu.A., Ushenko V.A., Dubolazov A.V., Balanetskaya V.O., Zabolotna N.I. Mueller-matrix diagnostics of optical properties of polycrystalline networks of human blood plasma. *Optics and Spectroscopy*. 2012. **112**, No. 6. P. 884–892.
24. Ushenko Yu.A., Tomka Yu.Ya., Dubolazov A.V. Laser diagnostics of anisotropy in birefringent networks of biological tissues in different physiological conditions. *Quantum Electronics*. 2011. **41**, No. 2. P. 170–175.
25. Ushenko Yu.A., Dubolazov A.V., Balanetskaya V.O., Karachevtsev A.O., Ushenko V.A. Wavelet-analysis of polarization maps of human blood plasma. *Optics and Spectroscopy*. 2012. **113**, No. 3. P. 332–343.
26. Ushenko Yu.A., Boychuk T.M., Bachynsky V.T., Mincer O.P. Diagnostics of structure and physiological state of birefringent biological tissues: Statistical, correlation and topological approaches. *Handbook of Coherent-Domain Optical Methods*. New York: Springer Science+Business Media, 2013. P. 107–148.
27. Ushenko Yu.A., Bodnar G.B., Koval G.D. Classifying optical properties of surface-and bulk-scattering biological layers with polarization singular states. *J. Innovative Opt. Health Sci*. 2013. **6**. P. 1350018.
28. Ushenko Yu.A. Statistical structure of polarization-inhomogeneous images of biotissues with different morphological structures. *Ukr. J. Phys. Opt*. 2005. **6**. P. 63–70.
29. Sroka R., Baumgartner R., Buser A., Ell C., Jocham D., Unsoeld E. Laser assisted detection of endogenous porphyrin in malignant diseases. *Proc. SPIE*. 1991. **1641**. P. 99–105.
30. D'Hallewin M.A., Kamuhabwa A.R., Roskams T., De Witte P.A., Baert L. Hypericin based fluorescence diagnosis of bladder carcinoma. *BJU Int*. 2002. **89**. P. 760–763.
31. D'Hallewin M.A., Bezdetnaya L., Guillemin F. Fluorescence detection of bladder cancer: a review. *Eur. Urol.* 2002. **42**. P. 417–425.